Accurate heteronuclear *J*-coupling measurements in dilute spin systems using the multiple-quantum filtered *J*-resolved experiment†

Charlotte Martineau,*[a] Franck Fayon,[b] Christophe Legein,[a] Jean-Yves Buzaré,[c] Gilles Silly[d] and Dominique Massiot[b]

Received (in Cambridge, UK) 5th March 2007, Accepted 3rd April 2007
First published as an Advance Article on the web 20th April 2007
DOI: 10.1039/b703321d

A new solid-state MAS NMR experiment is proposed to accurately measure heteronuclear ^{19}F–^{207}Pb *J*-coupling constants, even though these couplings are not visible on high speed ^{19}F 1D MAS spectra; in particular, we demonstrate that the *J*-resolved experiment combined with scalar multiple-quantum filtering considerably improves the resolution of *J*-multiplet patterns for dilute spin systems.

Scalar coupling in NMR is an important structural probe since the establishment of through bond connectivities and the corresponding *J*-coupling constant value provide detailed insights in the structure of crystalline or amorphous phases.[1] For example, the scalar interaction was proven to be very sensitive to internuclear distances,[2a] torsion angles[2b] or the ^{13}C–^{13}C bond order.[2c]

In rigid solids, *J*-couplings are often smaller than the resonance linewidth in magic angle spinning (MAS) NMR spectra which precludes an accurate measurement of the *J*-parameters. Therefore, efficient ways allowing the determination of *J*-coupling values are highly desirable. Recently, it was shown that homonuclear or heteronuclear *J*-couplings can be determined from two-dimensional MAS *J*-resolved experiments in crystalline or disordered solids for which the MAS linewidth can be several orders of magnitude larger than the *J*-coupling values.[3] These experiments rely on refocusing the inhomogeneous broadening due to the isotropic chemical shift distribution. However, when the observed nucleus is coupled to a dilute spin, the *J*-multiplet pattern is obscured by an intense singlet due to the presence of nuclei with nuclear spin $I = 0$. For homonuclear spin systems, it was shown that this difficulty can be overcome by inserting a double-quantum dipolar recoupling filter in the *J*-resolved experiment.[2c] In this contribution, we show that heteronuclear *J*-couplings between abundant and dilute spins in solids can be accurately measured using the *J*-resolved MAS experiment combined with scalar multiple-quantum filters. The experiment is applied to $Pb_5Ga_3F_{19}$ allowing the measurement of the ^{19}F–^{207}Pb *J*-couplings (^{207}Pb natural abundance: 22.6%) which are not resolved in the high spinning frequency MAS spectrum. We show that higher order multiple-quantum coherence filtering can be implemented in the experiment allowing the selection of higher order *J*-multiplet patterns.

$Pb_5Ga_3F_{19}$‡ results from the recrystallization of the transition-metal fluoride glasses PZG (PbF_2–ZnF_2–GaF_3). This compound and the PZG glasses were subject to numerous multinuclear NMR studies that led to a better understanding of the glass network structure.[4] The structure of $Pb_5Ga_3F_{19}$ is not well established, but it was assumed to be isostructural with $Pb_5Cr_3F_{19}$.[5] According to this assumption, the structure, based on a network of isolated and corner-sharing GaF_6^{3-} octahedra, involves two lead, two gallium and seven fluorine crystallographic sites (see ESI†). The fluorine ions can link two GaF_6^{3-} octahedra (shared fluorine), or belong to only one GaF_6^{3-} octahedron (unshared fluorine) or not belong to any GaF_6^{3-} octahedron ("free" fluorine). In $Pb_5Cr_3F_{19}$, in agreement with steric crowding arguments, the free and unshared fluorine sites exhibit short Pb–F bond lengths in the range 2.2–2.6 Å while the shared fluorine site shows a longer Pb–F distance at about 3.5 Å.

As shown in Fig. 1(a), the *J*-multiplet patterns due to ^{19}F–^{207}Pb *J*-couplings are not resolved in the ^{19}F high spinning frequency MAS spectrum§ of $Pb_5Ga_3F_{19}$. Nevertheless, evidence for the presence of ^{19}F–^{207}Pb *J*-couplings is indicated by the narrowing of the ^{19}F resonances under ^{207}Pb decoupling (Fig. 1(b)). The ^{19}F resonance linewidths measured in the ^{207}Pb-decoupled ^{19}F MAS

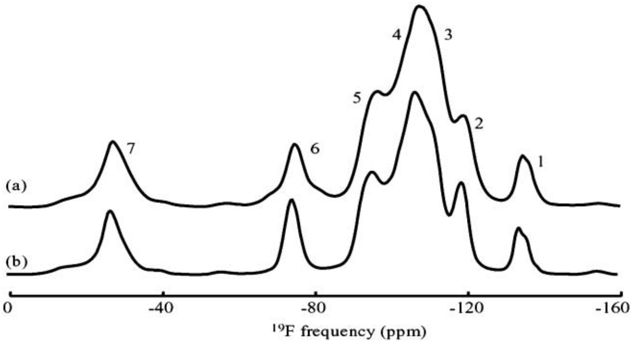

Fig. 1 Experimental§ ^{19}F MAS spectra of $Pb_5Ga_3F_{19}$ at spinning rate 30 kHz without (a) and with ^{207}Pb decoupling (b). ^{19}F resonances are labeled from 1 to 7.

---

[a] LdOF, CNRS UMR 6010, IRIM2F, CNRS FR 2575, Université du Maine, Avenue O. Messiaen, 72085, Le Mans Cedex 9, France. E-mail: charlotte.martineau.etu@univ-lemans.fr; Fax: +33 243833506; Tel: +33 243832627
[b] CRMHT, UPR CNRS 4212, 1D Avenue de la Recherche Scientifique, 45071, Orléans Cedex 2, France. E-mail: massiot@cnrs-orleans.fr
[c] LPEC, CNRS UMR 6087, IRIM2F, CNRS FR 2575, Université du Maine, Avenue O. Messiaen, 72085, Le Mans Cedex 9, France
[d] LPCMC, CNRS UMR 5617, Institut Charles Gerhardt, CNRS FR 1878, Université de Montpellier II, Place Eugène Bataillon, C.C. 3, 34095, Montpellier Cedex 5, France

† Electronic supplementary information (ESI) available: $Pb_5Cr_3F_{19}$ crystallographic data, experimental and reconstructed 1D ^{207}Pb decoupled ^{19}F MAS NMR spectra, 2D *J*-resolved and 2D multiple-quantum filtered *J*-resolved spectra of $Pb_5Ga_3F_{19}$ and the cross sections which are not shown in the paper. See DOI: 10.1039/b703321d

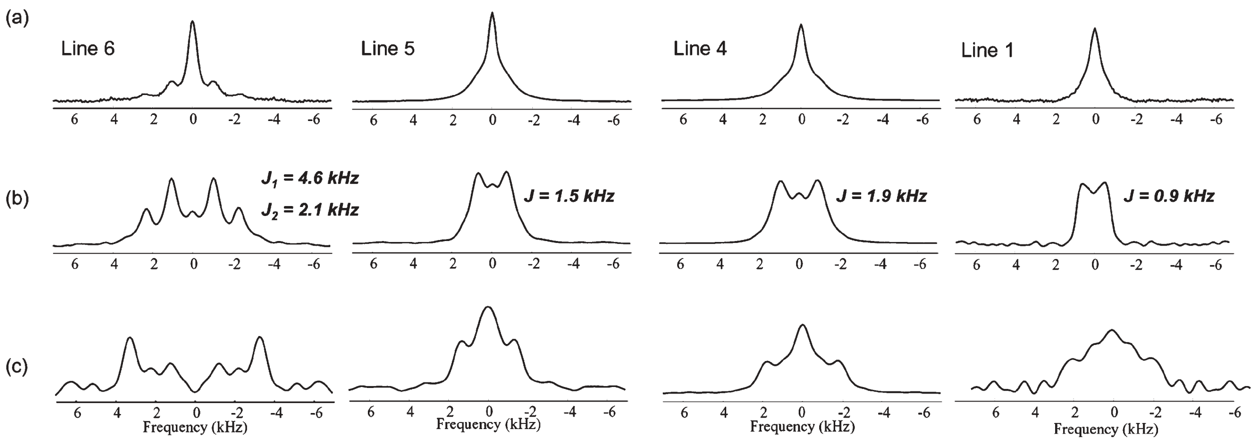

Fig. 2 Cross-sections of (a) 2D *J*-resolved, (b) ^{207}Pb single-quantum filtered 2D *J*-resolved and (c) ^{207}Pb double-quantum filtered 2D *J*-resolved MAS (30 kHz spinning frequency) spectra for ^{19}F resonances 1, 4, 5 and 6 of $Pb_5Ga_3F_{19}$. ^{19}F resonances 2, 3 and 7, shown in ESI,† exhibit similar *J*-patterns.

spectrum are of about 2 kHz, which is of the same order of magnitude as the ^{207}Pb–^{19}F *J*-coupling constants determined in α- and β-PbF_2 for which the *J*-coupling pattern is well resolved on the 1D ^{19}F MAS spectra.[6] A large part of the broadening of the ^{19}F resonances arises from the inherent low degree of crystallinity of this compound leading to a distribution of the ^{19}F isotropic chemical shift. This was supported by ^{19}F FSLG homonuclear decoupling experiments which did not improve the resolution in the ^{19}F 1D MAS spectrum. The ^{207}Pb-decoupled ^{19}F MAS spectrum can be fitted using seven lines with relative intensities in agreement with the proposed structure. As previously shown, "free" and shared fluorine ions have the highest and lowest isotropic chemical shifts, respectively.[4a] In between stand the unshared fluorine ions. On this basis, lines 1 and 7 are unambiguously assigned to the shared fluorine ion F7 and to the "free" fluorine ion F5, respectively, consistent with the relative line intensities. All other lines are relevant for the unshared fluorine ions and with regards to the line intensities, lines 2 and 6 would be assigned to F4 and/or F6, and lines 3, 4 and 5 to F1 and/or F2 and/or F3 (see ESI†).

As mentioned above, the broadening of the ^{19}F resonance linewidth is partly due to the inherent low degree of crystallinity of $Pb_5Ga_3F_{19}$. The 2D MAS *J*-resolved[3c] experiment§ allows to improve the resolution of the *J*-multiplet by refocusing the isotropic chemical shift distribution, as illustrated in Fig. 2(a). For each ^{19}F site, the observed lineshape is characteristic of a complex overlap of different *J*-multiplet patterns. Given the 22.6% ^{207}Pb natural abundance, each fluorine site has several $F(^{207}Pb)_x(Pb)_{n-x}$ magnetically inequivalent environments, where Pb represents the lead nuclei with no nuclear spin, and n is the number of Pb^{2+} ions in the first fluorine coordination sphere with $0 \leqslant x \leqslant n$. Therefore, each ^{19}F resonance is the sum of individual multiplets (for example, for $n = 3$, a singlet, a doublet, a triplet and a quadruplet) with relative intensities given by the probabilities for occurence of each of these environments. It should be mentioned that, while a contribution of the residual ^{19}F–^{19}F homonuclear dipolar couplings to the non-refocusable linewidth cannot be completely excluded, the short ^{19}F transverse dephasing in $Pb_5Ga_3F_{19}$ is believed to be mainly due to relaxation processes since we have observed fluorine motion in this compound through variable-temperature ^{19}F NMR experiments. The ^{19}F non-refocusable linewidth measured from the *J*-resolved spectrum recorded at 30 kHz is about 1 kHz, half the size of the linewidth in the ^{19}F MAS spectra. In that case, the presence of the intense central singlet prevents accurate *J*-coupling measurements.

To improve the resolution of the *J*-multiplet patterns we have combined the 2D *J*-resolved experiment with heteronuclear scalar multiple-quantum filtering[7] which allows the suppression of the ^{19}F singlet resonance. As shown in Fig. 3(a), the experiment, referred in the following as HMQC-filtered *J*-resolved, consists of a *J*-HMQC filter followed by a spin–echo sequence. As for the 2D *J*-HMQC correlation experiment,[8] the τ delays are synchronized with the rotor period. After the second delay τ, a ^{207}Pb 90° pulse is applied to convert the remaining anti-phase coherences into multiple-quantum coherences before the incremented t_1 spin echo period. It may be omitted if $\tau = 1/(2J)$. Then, the ^{19}F HMQC-filtered in-phase coherences evolve under the heteronuclear scalar coupling, the isotropic chemical shift being refocused by the simultaneous 180° pulses on both nuclei. Selected cross sections of the 2D HMQC-filtered *J*-resolved spectrum§ (see ESI†) of $Pb_5Ga_3F_{19}$ obtained using a ^{207}Pb single-quantum filter are shown Fig. 2(b). The increased resolution of the doublet due to the suppression of the intense singlet resonance is clearly shown. Higher order *J*-multiplets of weaker intensities are also evidenced on both sides of the doublet. Selection of these higher order *J*-multiplets can be achieved using a ^{207}Pb higher coherence order

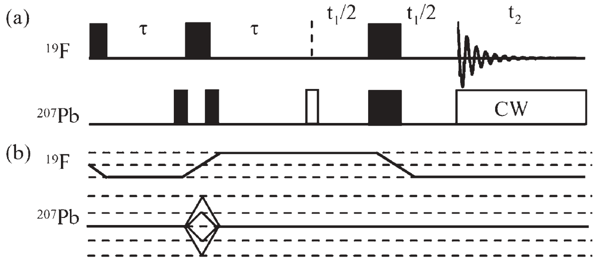

Fig. 3 (a) Pulse sequence and (b) coherence pathways for the HMQC-filtered *J*-resolved experiments. The delays τ were synchronized with the rotor period. The phases of the two ^{19}F 180° pulses were cycled by steps of 90° to select the desired echo pathway. ^{207}Pb single- or double-quantum filtering was achieved by cycling the phases of the ^{207}Pb 90° pulses by steps of 180 and 90°, respectively.

Table 1 Line label, line attribution and ^{207}Pb–^{19}F *J*-coupling constants for $Pb_5Ga_3F_{19}$, as deduced from the MAS HMQC-filtered *J*-resolved spectra

Line	1	2	3	4	5	6	6	7
Attribution	F7	F4 or F6	F1 or F2 or F3			F4 or F6		F5
J/kHz	0.9	1.9	1.5	1.9	1.5	4.6	2.1	2.0

filter (Fig. 3(b)). As illustrated in Fig. 2(c), the *J*-resolved spectrum obtained using a ^{207}Pb double-quantum filter allows to suppress both the singlet and the doublet resonances and to clearly observe the higher order *J*-multiplets from which *J*-coupling constants are extracted as well. To maximize the filtering efficiency of a given coherence order, the delay τ was optimized depending on the size of the spin system and the *J*-coupling values.[7] The delay τ of the scalar filter can also be adjusted to enhance the signal of a selected range of *J*-couplings. In principle, the use of the highest coherence order filter allows probing the total number of lead atoms bonded to each fluorine ion. However, in $Pb_5Ga_3F_{19}$, the detection of ^{207}Pb coherence orders higher than two is difficult due to both the relatively low ^{207}Pb natural abundance (22.6%) and the rapid ^{19}F transverse dephasing.

In the HMQC filtered *J*-resolved spectra of $Pb_5Ga_3F_{19}$, *J*-coupling multiplets are clearly resolved for each fluorine sites. Assuming $Pb_5Ga_3F_{19}$ is isostructural with $Pb_5Cr_3F_{19}$, each fluorine ion is surrounded by several lead atoms with different F–Pb internuclear distances for which different *J*-coupling constants are expected. However, for all resonances except line 6, the *J*-resolved spectrum with ^{207}Pb single-quantum filtering evidences a single broad doublet from which average *J*-coupling values, ranging from 0.9 to 2.0 kHz (Table 1), are extracted. Similarly, a broad triplet pattern is observed for these resonances in the ^{207}Pb double-quantum filtered *J*-resolved spectrum. For resonance 7, assigned to the "free" fluorine F5, we measure an average *J*-coupling constant of 2.0 kHz, very similar to that reported for α-PbF_2.[6a,b] For the resonances attributed to the unshared fluorine ions, most of the values are smaller than that of the "free" fluorine. For the shared fluorine F7 (line 1), which has longer Pb–F distances of about 3.5 Å, a significantly weaker *J*-coupling constant of 0.9 kHz is measured. This highlights the sensitivity of the *J*-coupling to Pb–F internuclear distances. In the case of the resonance 6 (assigned to either F4 or F6), the *J*-resolved spectra recorded with ^{207}Pb single- and double-quantum filtering show two significantly different *J*-coupling values of 4.6 and 2.1 kHz. Considering the *J*-coupling values measured for all other resonances and the high isotropic chemical shift for this unshared fluorine, this particularly strong *J*-coupling constant would indicate a much shorter F–Pb bond length. However, this is not consistent with the structure of $Pb_5Cr_3F_{19}$ in which the unshared fluorine sites F4 or F6 do not exhibit a very short Pb–F distance. Neutron diffraction experiments are currently carried out to precisely determine F–Pb distances in $Pb_5Ga_3F_{19}$. Then, we expect to be able to correlate *J*-coupling constants and interatomic distances.

In this communication, we have proposed a new HMQC-filtered *J*-resolved NMR experiment that allows measuring heteronuclear *J*-coupling constants in solids for dilute spin systems. The use of scalar multiple-quantum filters considerably improves the resolution of the *J*-resolved experiment by removing the intense singlet due to the dilute nuclei. Applied to $Pb_5Ga_3F_{19}$, the range of measured ^{19}F–^{207}Pb scalar couplings reflects the high sensitivity of the *J*-coupling to the F–Pb internuclear distance.

Notes and references

‡ $Pb_5Ga_3F_{19}$ was synthesized from solid-state reaction of a stoichiometric mixture of PbF_2 and GaF_3 in sealed platinum tubes. These starting materials being moisture sensitive, all operations of weighing, mixing and grinding were done in a dry glove-box, under nitrogen atmosphere. The stoichiometric mixture was heated at 520 °C for 6 days and naturally cooled. The purity of the obtained phase was checked by X-ray powder diffraction method against the PDF file number 47–0287.

§ All NMR experiments were recorded on an Avance 400 Bruker spectrometer operating at ^{19}F and ^{207}Pb Larmor frequencies of 376.54 and 83.72 MHz, respectively. A high speed (up to 35 kHz) ^{19}F optimized CP MAS probe with a 2.5 mm rotor was used. $CFCl_3$ was used as external reference for ^{19}F. The spectra were recorded at a spinning frequency of 30 kHz and the sample temperature was monitored to 28 °C using a Bruker cooling unit. The ^{207}Pb isotropic chemical shift of $Pb(NO_3)_2$ was used as an NMR thermometer.[9] 2.15 μs 90° pulse (RF field of 100 kHz) and 2.25 μs 90° pulse (RF field of 90 kHz) were used for ^{19}F and ^{207}Pb, respectively. Recycle delays were taken to 1 s. The delays τ were synchronized with the rotor period and set to 150 and 300 μs in the HMQC-filtered *J*-resolved experiments employing a ^{207}Pb single quantum and double quantum filter, respectively. When specified, ^{207}Pb continuous wave decoupling with an RF field strength of about 70 kHz was used during the signal acquisition. The ^{207}Pb decoupled ^{19}F MAS spectrum was reconstructed using the DMFit[10] software and the corresponding parameters are given in ESI.†

1 J. Varaa, J. Jokisaari, R. E. Wasylishen and D. L. Bryce, *Prog. Nucl. Magn. Reson. Spectrosc.*, 2002, **41**, 233.

2 (*a*) M. Karplus, *J. Am. Chem. Soc.*, 1963, **85**, 2870; (*b*) J. S. Hu, S. Grzesiek and A. Bax, *J. Am. Chem. Soc.*, 1997, **119**, 1803; (*c*) W. C. Lai, N. McLean, A. Gansmüller, M. A. Verhoeven, G. C. Antonioli, M. Carravetta, L. Duma, P. H. M. Bovee-Geurts, O. G. Johannessen, H. J. M. de Groot, J. Lugtenburg, L. Emsley, S. P. Brown, R. C. D. Brown, W. J. DeGrip and M. H. Levitt, *J. Am. Chem. Soc.*, 2006, **128**, 3878.

3 (*a*) G. Wu and R. E. Wasylishen, *Inorg. Chem.*, 1992, **31**, 145; (*b*) S. P. Brown, M. Perez-Torralba, D. Sanz, R. M. Claramunt and L. Emsley, *Chem. Commun.*, 2002, 1852; (*c*) A. Lesage, L. Emsley, M. Chabanas, C. Copéret and J.-M. Basset, *Angew. Chem., Int. Ed.*, 2002, **41**, 4535; (*d*) F. Fayon, I. J. King, R. K. Harris, J. S. O. Evans and D. Massiot, *C. R. Chim.*, 2004, **7**, 351; (*e*) S. P. Brown and L. Emsley, *J. Magn. Reson.*, 2004, **171**, 43.

4 (*a*) B. Bureau, G. Silly, J.-Y. Buzaré, J. Emery, C. Legein and C. Jacoboni, *J. Phys.: Condens. Matter*, 1997, **9**, 6719; (*b*) B. Bureau, G. Silly, J.-Y. Buzaré, C. Legein and D. Massiot, *Solid State Nucl. Magn. Reson.*, 1999, **14**, 181; (*c*) B. Bureau, G. Silly and J.-Y. Buzaré, *Solid State Nucl. Magn. Reson.*, 1999, **15**, 79.

5 J. Ravez, V. Andriamampianina, A. Simon, J. Grannec and S. C. Abrahams, *J. Appl. Phys.*, 1991, **70**, 1331.

6 (*a*) F. Wang and C. P. Grey, *J. Am. Chem. Soc.*, 1995, **117**, 6637; (*b*) F. Wang and C. P. Grey, *J. Am. Chem. Soc.*, 1998, **120**, 970; (*c*) R. E. J. Sears, Q. Zh. Guo and H. J. Mackey, *J. Chem. Phys.*, 1984, **80**, 5448.

7 D. Sakellariou, A. Lesage and L. Emsley, *J. Magn. Reson.*, 2001, **151**, 40.

8 A. Lesage, D. Sakellariou, S. Steuernagel and L. Emsley, *J. Am. Chem. Soc.*, 1998, **120**, 13194.

9 (*a*) L. C. M. van Gorkom, J. M. Hook, M. B. Logan, J. V. Hanna and R. E. Wasylishen, *Magn. Reson. Chem.*, 1995, **33**, 791; (*b*) A. Bielecki and D. P. Burum, *J. Magn. Reson., Ser. A*, 1995, **116**, 215.

10 D. Massiot, F. Fayon, M. Capron, I. King, S. Le Calvé, B. Alonso, J. O. Durand, B. Bujoli, Z. Gan and G. Hoatson, *Magn. Reson. Chem.*, 2002, **40**, 70.